Front. Phys. China, 2009, 4(3): 408–414
DOI 10.1007/s11467-009-0034-6

RESEARCH ARTICLE

# Structural and magnetic properties of bimetallic $Co_{n-1}Cr$ clusters with density functional theory

**Nai-feng SHEN** (沈乃丰), **Yan-biao WANG** (王彦彪), **Sheng CHEN** (陈昇), **Jin-lan WANG** (王金兰)(✉)

*Department of Physics, Southeast University, Nanjing 211189, China*
*E-mail: jlwang@seu.edu.cn*

*Received January 14, 2009; accepted February 25, 2009*

We have investigated the structural and magnetic properties of small bimetallic $Co_{n-1}Cr$ ($n = 2-9$) clusters by means of spin-polarized density functional theory approach. We found the ground state structures of $Co_{n-1}Cr$ were very similar to those of pure $Co_n$ except $n = 3, 6$. The clusters were of high stability at $n = 6$. Magnetic moments showed an interesting size-dependent variation: the magnetic moments of $Co_{n-1}Cr$ can be obtained by minus $7\mu_B$ for $n = 2, 4, 6$–$9$ or by plus $1\mu_B$ for $n = 5$ from those of the $Co_n$ counterparts. The different magnetic behavior stems from ferromagnetic alignment or ferrimagnetic alignment of Co and Cr atoms in $Co_{n-1}Cr$, associated with their longer or shorter interatomic distances.

**Keywords** bimetallic culsters, magnetism, density functional theory

**PACS numbers** 75.75.+a, 61.46.Bc, 73.22.-f, 36.40.Cg

## 1 Introduction

Small transition metal (TM) clusters that aggregates of a few to a few tens atoms or molecules have attracted enormous interest either from basic–science or application point of view in the past few decades. Due to the large surface–volume ratio, finite size effect, and quantum size effect, they often exhibit quite different structural and magnetic properties from their corresponding bulk. Bimetallic TM clusters are of particular interest because the properties are tunable even by changing their chemical compositions. Besides, the heterogeneous magnetic structures offer opportunities for cluster-assembled materials with new functions for magnetic recording and medical applications [1, 2]. To date, a few studies have been made on the structural and magnetic properties of cobalt-based bimetallic TM clusters [3–11]. Experimentally, magnetic deflection study of $Co_nBi_m$ suggested that the clusters adopt segregated structures with ferromagnetic $Co_n$ "cores" surrounded by the Bi atom shell [3]. Stern–Gerlach molecular beam deflection experiments show that the magnetic moments of $Co_NMn_M$ increase with Mn concentration, while those of $Co_NV_M$($N \leqslant 60$; $M \leqslant N/3$) decrease as V doping [4]. The $Co_NMn_M$ ($N + M = 11$–$29$) were also found to have same magnetic moments as those of pure Co clusters with the same total number of atoms [5]. Theoretically, different level computational techniques including genetic algorithm combined tight-binding molecular dynamics method and first-principle method have been exploited on studying the structures and magnetism of Co-based bimetallic clusters. Segregated layered structures were predicted computationally in the Co–Cu bimetallic clusters, and their magnetic moments decrease with the increase of Cu atoms [6]. The $Co_mPt_n$ ($n+m = 38$) clusters mostly adopt icosahedral conformations with their average magnetic moments per atom decrease with Pt concentration as compared to those of the pure $Co_{38}$ cluster [7]. The magnetic moments of icosahedral $TMCo_{12}$, M = Ti, V, Cr, Mn, Fe, Ni, clusters were reduced when a Co atom is replaced with a TM atom [8]. Small bimetallic $Mn_xCo_y$ ($x+y = 2$–$5$, $x = 0$–$n$) clusters show insensitive magnetic dependence to cluster size and composition [9]. Most recently, the magnetic properties of Co–Mn and Co–V clusters were investigated [10, 11]. Moreover, the magnetic enhancement or reduction were identified upon Mn or V substitution, compared to pure $Co_n$, consistent with recent experimental [5] observation in large-sized clusters.

In this paper, we have performed spin-polarized *ab ini-*

*tio* pseudopotential plane wave density functional theory (DFT) to investigate the size-dependent structural and magnetic properties of bimetallic $Co_{n-1}Cr$, $n$ = 2–9 clusters. We found that the $Co_{n-1}Cr$ clusters were of high stability at $n$=6 and showed an interesting size-dependent variation in magnetic moments: the magnetic moments of $Co_{n-1}Cr$ is reduced by $7\mu_B$ for $n$=2, 4, 6–9 and increase by $1\mu_B$ for $n$=5 as compared with those of the pure $Co_n$clusters. The different magnetic behavior was attributed to ferromagnetic alignment or ferrimagnetic alignment of Co and Cr atoms in $Co_{n-1}Cr$, which is induced by their elongated or shortened bond lengths in the bimetallic clusters.

## 2 Computational method

All the calculations were carried out by means of *ab initio* pseudopotential plane wave DFT implemented in the Vienna Ab initio Simulation Package (VASP) [12]. The electron–core interaction was described by projected augmented wave (PAW) pseudopotential [13, 14] within the general gradient approximation (GGA) parameterized by Perdew, Burke, and Ernzerhof (PBE) [15]. In the optimization, the cluster was placed in a cubic cell with edge length of 15 Å to ensure that interaction between the supercells negligible. The energy cutoff in the plane-wave expansion of the pseudowavefunctions was set to 350 eV, and the calculations were performed at the gamma-point only. All structures were fully optimized without symmetry constrain using a conjugate-gradient algorithm until the Hellmann–Feynman force acting on each atom was less than 0.005 eV/Å.

The accuracy of PBE/PAW combination is justified by the smallest $Co_2$, $Cr_2$, and CoCr dimers, as displayed in Table 1. The results obtained from PBE/PAW are in good agreement with earlier computations and the measured values [16–19]. Therefore, this PBE/PAW combination is expected to give a good description of Co–Cr bimetallic clusters.

**Table 1** Comparison of our DFT results with experimental (EXP) studies and other theoretical calculations for CoCr, $Co_2$, nd $Cr_2$, where $E_b$ and $R_c$ are the binding energy per atom and bond length, respectively.

| System | Methods | Bond length/Å | | | Average binding energy | | |
|---|---|---|---|---|---|---|---|
| | | Ours | Others | EXP | Ours | Others | EXP |
| $Co_2$ | PBE | 1.964 | 1.96[a] | 2.31[b] | 1.455 | 1.45[a] | 1.72[b] |
| | LDA | 1.908 | | | 2.419 | | |
| | PW91 | 1.960 | | | 1.521 | | |
| $Cr_2$ | PBE | 1.512 | 1.72[d] | 1.68[d] | 0.987 | 0.71[d] | 0.72[d] |
| | LDA | 1.461 | | | 2.258 | | |
| | PW91 | 1.509 | | | 1.447 | | |
| CoCr | PBE | 2.350 | 2.34[c] | – | 0.824 | 0.67[c] | – |
| | LDA | 1.763 | | | 1.507 | | |
| | PW91 | 2.238 | | | 1.073 | | |

[a−d]From Refs. [16–19].

To locate the ground-state structures of bimetallic clusters, we considered a number of different configurations including linear chains, planar, and three-dimensional structures. We constructed all the possible structures of $Co_{n-1}Cr$ ($n$ = 2–9) based on our earlier studies on $Co_n$, $Co_{n-1}Mn$, and $Co_{n-1}V$. To reduce the number of independent structures, we set it to the closest symmetry without changing its packing; that is, we used a loose symmetry criterion for the clusters and substituted a Co/Mn/V atom with a Cr atom in various positions. To obtain the ground spin states, two steps were taken: the magnetic moment was first allowed to optimize freely to the energetically favored spin state ($S_z$); then, the neighboring spin states ($S_z \pm 2$) were fixed during the optimization to ensure that the obtained spin state is the most energetically preferred. This procedure has been successfully identified the ground-state structure of Co–Mn and Co–V bimetallic clusters in our recent work [11].

## 3 Results and discussion

### 3.1 Equilibrium geometry

The optimized low-energy structures of the $Co_{n-1}Cr$ clusters are displayed in Fig. 1, together with the magnetic moment and energy ($\Delta E$) relative to the lowest energy structure. The ground-state structures of $Co_n$ were also included for comparison.

The bond length and the binding energy of CoCr were 2.41 Å and 0.65 eV per atom, respectively, close to earlier DFT results (2.34 Å, 0.67 eV) [18]. For $Co_2Cr$, a triangle and a linear chain were taken into account, and the lowest energy structure was an isosceles triangle with $C_{2v}$ symmetry. We considered a three-dimensional (3-D) tetrahedron and a planar square for $Co_3Cr$ and found the most stable structure is the planar rhombus structure in a quartet state; another rhombus structure in a doublet state 0.079 eV higher in energy, while the tetrahedral structure possesses much high energy ($\Delta E$ = 0.727 eV). For the case of $Co_4Cr$, we considered the triangular bipyramid, singly square pyramid, and planar W-shape structures as initial conformations for geometry optimization. The triangular bipyramid with the Cr atom located on the interface planar triangle was found most energetically preferred.

Considering the linear and planar structures are much less stable both in $Co_n$ and $Co_{n-1}Cr$, only 3D compact structures were taken into consideration for the geometry optimization for large-sized clusters with $n \geqslant 6$. Therefore, for $Co_5Cr$, we constructed a singly capped triangular bipyramid, an octahedron, and a pentagonal pyramid as initial structures; the energetically favorable is the distorted octahedron in $C_s$ symmetry having magnetic mo-

(a) $D_{infv}$, $3\mu_B$, 0 (b) $D_{infv}$, $5\mu_B$, 0.495 eV

(a) $D_{2v}$, $2\mu_B$, 0 (b) $C_{2v}$, $0\mu_B$, 0.024 eV (c) $D_{infh}$, $0\mu_B$, 0.35 eV

(a) $C_s$, $3\mu_B$, 0 (b) $C_{2v}$, $1\mu_B$, 0.079 eV (c) $C_s$, $7\mu_B$, 0.727 eV

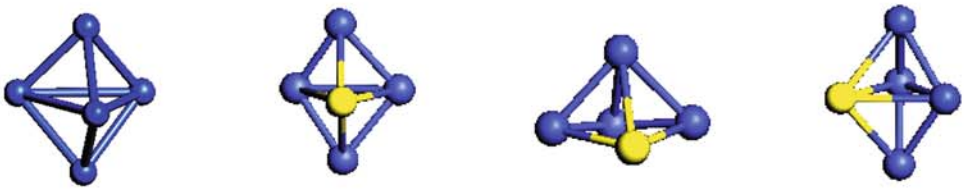

(a) $C_s$, $14\mu_B$, 0 (b) $C_s$, $6\mu_B$, 0.028 eV (c) $C_{2v}$, $12\mu_B$, 0.27 eV

(d) $C_{3v}$, $12\mu_B$, 0.41 eV

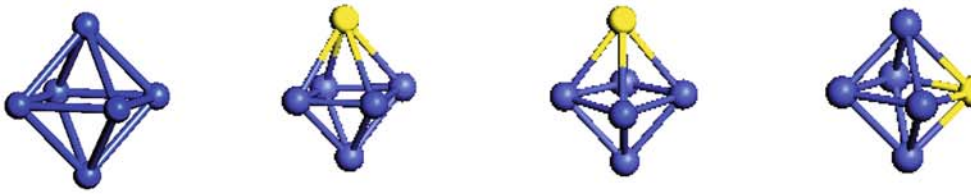

(a) $C_s$, $7\mu_B$, 0 (b) $C_{2v}$, $17\mu_B$, 0.039 eV (c) $C_s$, $13\mu_B$, 0.141 eV

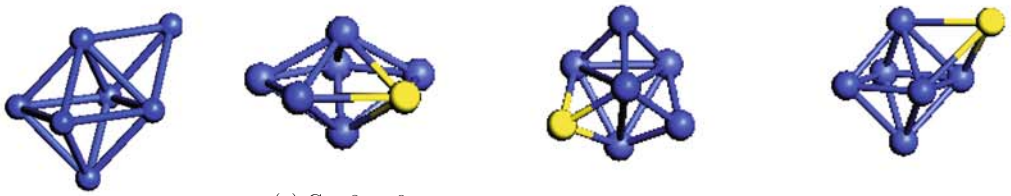

(a) $C_{2v}$, $8\mu_B$, 0 (b) $C_s$, $8\mu_B$, 0.11 eV (c) $C_s$, $18\mu_B$, 0.121 eV

(d) $C_{3v}$, $8\mu_B$, 0.188 eV (e) $C_{5v}$, $8\mu_B$, 0.227 eV (f) $C_s$, $8\mu_B$, 0.375 eV

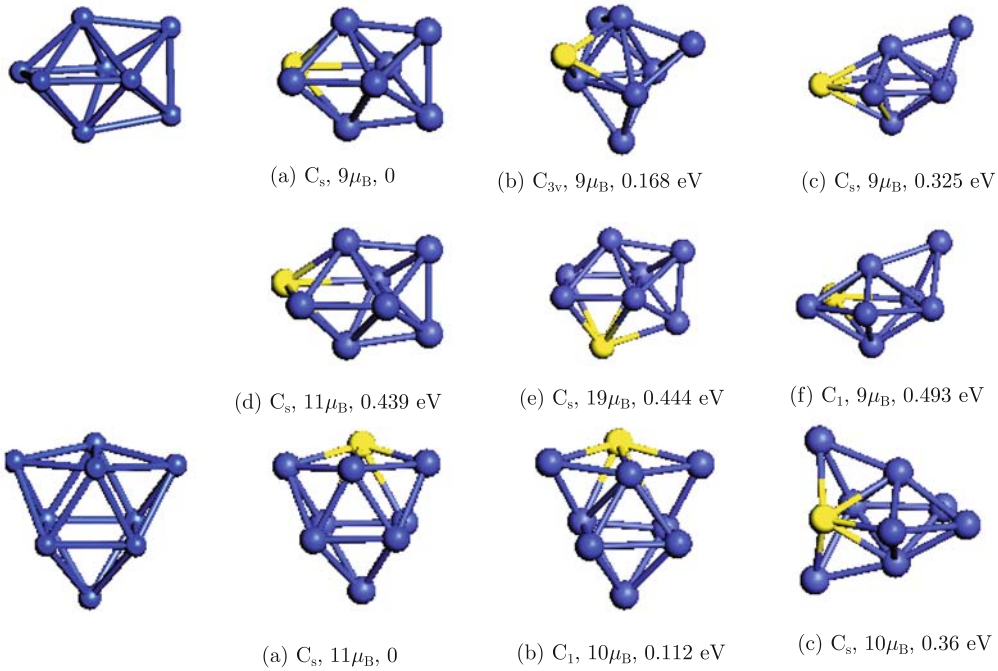


**Fig. 1** Lowest energy and low-lying structures of $Co_{n-1}Cr$ ($n = 2$–9). The blue and yellow balls represent Co and Cr, respectively.

ment of $7\mu_B$. The higher magnetic states of 17 and $13\mu_B$ possess a little higher energy above the ground state one by 0.039 and 0.141 eV, respectively. As for $Co_6Cr$, we considered the bicapped triangular bipyramid, capped octahedron, pentagonal bipyramid, and hexagonal pyramid structures as initial structures for geometry optimization. Different from $Co_7$, $Co_6Mn$, and $Co_6V$, the pentagonal bipyramid instead of the capped octahedron was identified as the most energetically favored structure with the magnetic moment of $8\mu_B$. The bicapped triangular bipyramid follows with 0.11 eV higher in energy. The capped octahedron was found to be 0.121 eV less stable than the ground-state structure. Three other isomers with even higher energies were also located, as shown in Fig. 1. For the case of $Co_7Cr$, we considered four different initial geometries, a tricapped triangular bipyramid, a bicapped octahedron, a capped pentagonal bipyramid, and a hexagonal bipyramid for geometry optimization. The bicapped octahedron is the most stable, followed by the tricapped triangular bipyramid and the capped pentagonal bipyramid with 0.168 and 0.325 eV higher energy with respect to the ground state one. All these three structures have the same value magnetic moment of $9\mu_B$. The largest cluster in the work is $Co_8Cr$, while its lowest energy structure is the singly capped anti-four-prism structure having $C_s$ symmetry with a magnetic moment of $10\mu_B$. The tricapped octahedron and the bicapped pentagonal bipyramid structures lie 0.11 and 0.36 eV higher in energy above the lowest energy structure, respectively.

As discussed above, the ground state structures of $Co_{n-1}Cr$ are close to those of pure $Co_n$, with the exception of $Co_3Cr$ and $Co_6Cr$, which the tetrahedral structure and singly capped octahedron structures are found for $Co_n$ clusters. On the other hand, the rhombus structure and the pentagonal bipyramid structure are for $Co_{n-1}Cr$ clusters.

### 3.2 Binding energy and relative stability

To investigate the stability and size-dependent behavior of the cluster, we computed the average binding energies (BEs) per atom of the lowest energy structures of the $Co_{n-1}Cr$ clusters, $E_b(n)$, and the second difference in energy, $\Delta_2 E(n)$, defined as:

$$E_b(n) = \{(n-1)E[\mathrm{Co}] + E[\mathrm{M}] - E[\mathrm{Co}_{n-1}\mathrm{M}]\}/n \quad (1)$$

$$\Delta_2 E(n) = E[\mathrm{Co}_{n+1}\mathrm{M}] + E[\mathrm{Co}_{n-1}\mathrm{M}] - 2E[\mathrm{Co}_n\mathrm{M}] \quad (2)$$

in which $E[\cdot]$ is total energy of the relaxed $Co_{n-1}Cr$ clusters, isolated Co atom, and Cr atom.

As displayed in Fig. 2(a), the BEs of $Co_{n-1}Cr$ and $Co_n$ both increase monotonically with cluster size. The BE of $Co_{n-1}Cr$ is always lower than that of the pure $Co_n$ clusters, suggesting that doping Cr into the $Co_n$ clusters reduces the stability of the clusters. Moreover, the BE curves can be divided into two stages: the BEs show rapid increase in the range of $n = 2-6$ and rather smooth increase thereafter, implying the clusters at $n = 6$ might be of high stability. This is clearly classified in Fig. 3(b), with extremely high peaks of $\Delta_2 E(n)$ being observed at $n = 6$. The high stability of the $Co_5Cr$ and $Co_6$ clusters may stem from their compact octahedron structures, while the ground state structures of $n = 7$ can be ob-

tained by capping an atom on the octahedrons, which weakens the stability of the clusters.

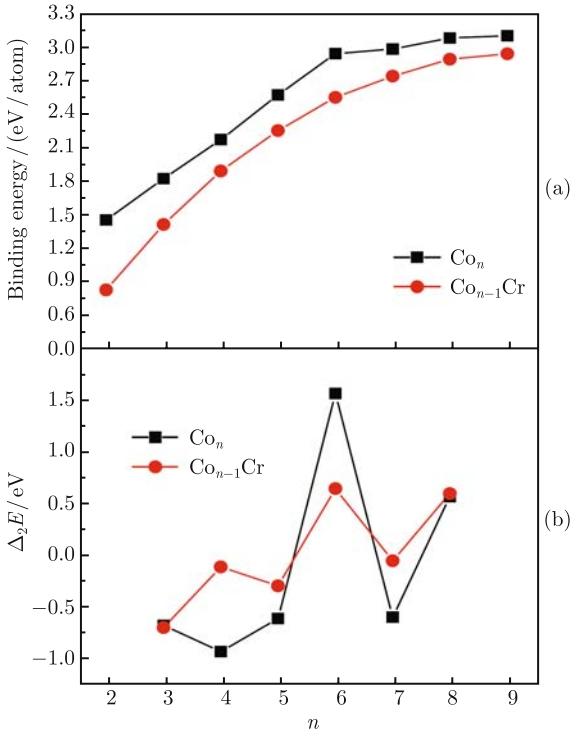


**Fig. 2** **(a)** Average binding energy per atom of the lowest energy structure; **(b)** Second energy difference of $Co_{n-1}Cr$ and $Co_n$.

### 3.3 Size-dependent magnetic moments

The total magnetic moments of the lowest energy structures of $Co_{n-1}Cr$ and $Co_n$ are plotted in Fig. 3 as functions of cluster size. The magnetic moment of $Co_n$ increases monotonically with cluster size, while that of $Co_{n-1}Cr$ shows a complicated size-dependent variation. The magnetic moment decreases from $3\mu_B$ of CoCr to $2\mu_B$ of $Co_2Cr$ and increases up to $14\mu_B$ at $Co_4Cr$. The magnetic moment decreases again thereafter to $7\mu_B$ of $Co_5Cr$ and increases with the increase of cluster size. Most interestingly, the magnetic moment of $Co_{n-1}Cr$ decreases significantly by $7\mu_B$ at $n = 2, 4, 6$–9 and increases by $1\mu_B$ in $Co_4Cr$ upon Cr doping compared to that of the corresponding $Co_n$ counterparts.

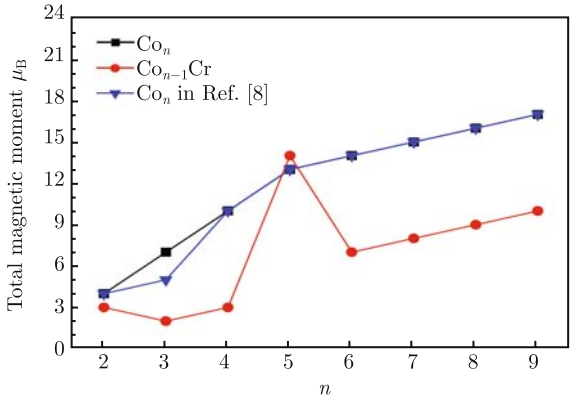


**Fig. 3** Total magnetic moments of the most stable structures of $Co_{n-1}Cr$ and $Co_n$, $n = 2$–9.

To gain more insight into the complicated magnetic behaviors of Co–Cr clusters, we investigated local atomic magnetic moments shown in Fig. 4, computed from the difference of the local spin up and down charges by integrating the projected charge densities inside the volume of a sphere centered at the atoms' site of the lowest energy structure of $Co_{n-1}Cr$. The local magnetic moments on Cr and Co atoms are around 4.0 and $2.0\mu_B$, respec-

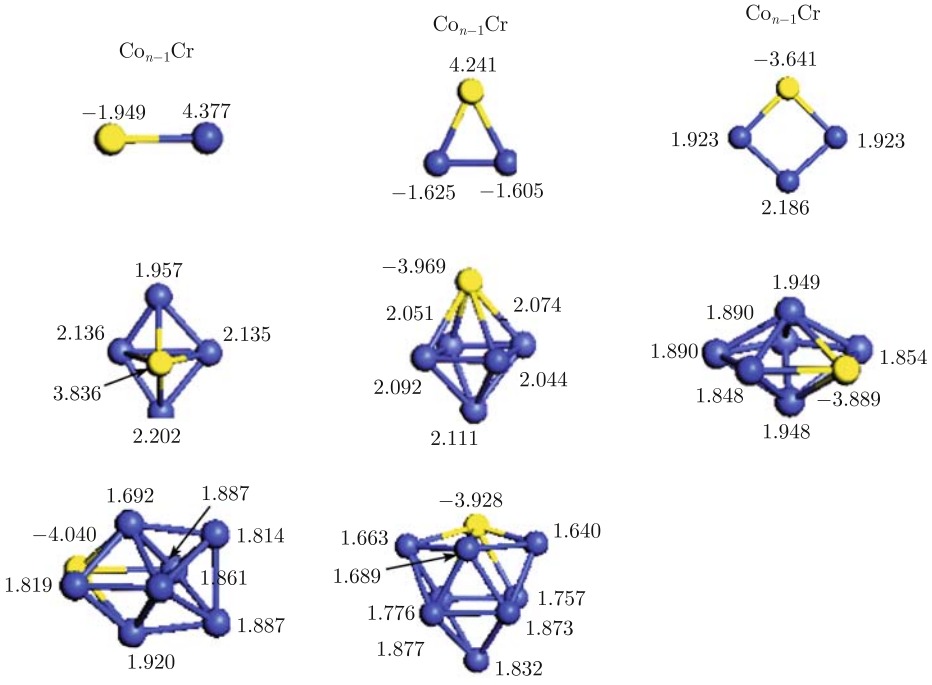


**Fig. 4** Local magnetic moment of the most stable structures of $Co_{n-1}Cr$, $n = 2$–9.

tively. Ferromagnetic ordering, namely, the spins on each atom being all parallel, was identified for $Co_4Cr$, while a ferrimagnetic state in which the spins on the Cr atom were antiparallel to those on the Co atoms for the rest, was found. Therefore, the magnetism of the cluster was enhanced upon Cr doping at $n = 5$ and was attenuated by Cr doping for others.

Their different magnetic behaviors of the clusters can be further understood in light of their electronic and geometric features. On one hand, the ground electronic configurations of isolated Cr and Co are $3d^54s^1$and $3d^74s^2$, that is, each atom can have atomic magnetic moments as large as 6 and $3\mu_B$, respectively. Considering the ferromagnetic alignment in $Co_n$ and the ferrimagnetic ordering for $Co_{n-1}Cr$ (except $n = 5$), their unpaired electrons according to Hund's rule will be $3n$ and $3n$–7, respectively. Thus, the magnetic moments of the $Co_{n-1}Cr$ bimetallic clusters decrease by $7\mu_B$ for $n$ = 2, 4, 6–9. On the contrast, due to interaction between atoms, the local moments on each atom may be reduced more or less, as compared with the ideal isolated atomic values. On the contrast, the Cr atom is ferromagnetic coupling with Co atoms in $Co_4Cr$, and the local magnetic moment on Cr is about $4.0\mu_B$, which results in its total magnetic moment is enhanced by $1\mu_B$ compared to that of $Co_5$. On the other hand, the distinct magnetic behavior of the $Co_{n-1}Cr$ clusters appears to correlate with their structural characteristics, such as trend of average bond length of the clusters. We depicted the bond length of $Co_{n-1}Cr$ clusters in Fig. 5. One can clearly see from the figure that the cluster $Co_4Cr$ has the largest average bond length among all the sizes studied in this work. The large bond length in this cluster may be responsible for its largest magnetic moment. Previous DFT studies have also shown that the lengthening of the interatomic distances leads to a magnetic transition from antiferromagnetic or ferrimagnetic state to ferromagnetic state accompanying an increase of the local magnetic moments in iron clusters and $[Mn_{13}@Au_{20}]^-$ clusters [20, 21], which eventually results in the large total magnetic moment of the cluster.

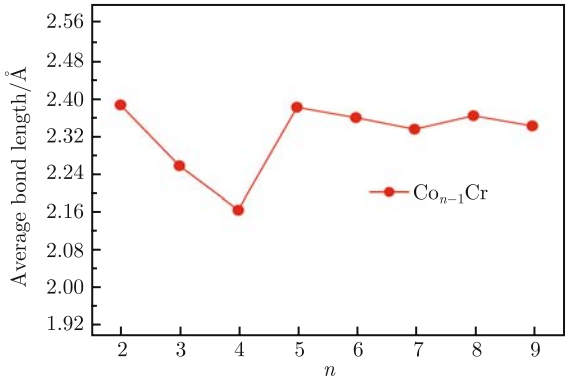


**Fig. 5** Average bond length of the lowest energy structure of $Co_{n-1}Cr$, $n$ = 2–9.

### 3.4 Spin gaps and spin stability

The spin gaps, $\delta_1$ and $\delta_2$ defined as

$$\delta_1 = -(\varepsilon_{\mathrm{HOMO}}^{\mathrm{majority}} - \varepsilon_{\mathrm{LUMO}}^{\mathrm{minority}})$$

$$\delta_2 = -(\varepsilon_{\mathrm{HOMO}}^{\mathrm{minority}} - \varepsilon_{\mathrm{LUMO}}^{\mathrm{majority}})$$

are often used to evaluate the spin stability of the cluster theoretically. Generally, a given spin arrangement is classified as magnetic stable if $\delta_1$ and $\delta_2$ are both positive. More precisely, magnetic stability occurs when the LUMO of the majority manifolds (spin-up) lies above the HOMO of the minority (spin-down) manifolds, and vice versa. The spin gaps $\delta_1$ and $\delta_2$ of the ground state structures of the $Co_{n-1}Cr$ ($n$ = 2–9) clusters are depicted in Fig. 6. The $\delta_2$ possesses larger values than $\delta_1$ with the exception of $n$ = 8, 9. Moreover, it was clearly found that both $\delta_1$ and $\delta_2$ were positive for all the cases, indicating that all the clusters studied in this article were magnetic stable.

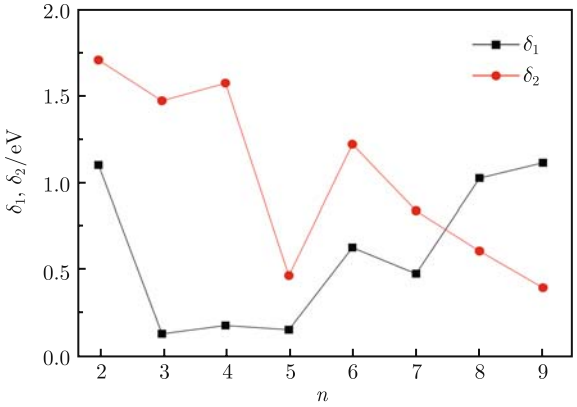


**Fig. 6** Spin gaps as functions of cluster size $n$ are plotted for $Co_{n-1}Cr$, $n$ = 2–9.

## 4 Conclusion

In summary, we have carried out spin-polarized density functional theory calculations on the bimetallic $Co_{n-1}Cr$, $n$ = 2–9, clusters and investigated their size-dependent energetic and magnetic properties. The most stable structures of $Co_{n-1}Cr$ were similar to those of $Co_n$ except $Co_3Cr$ and $Co_6Cr$. The clusters exhibited high stability at $n = 6$. The magnetic moment increased by $1\mu_B$ when substituting a Co atom with a Cr atom at $n = 5$, whereas it was reduced by $7\mu_B$ upon Cr doping for the rest with the exception of $Co_2V$. The different magnetic behaviors in $Co_{n-1}Cr$ were also associated with their geometric features. The longer bond lengths in $Co_4Cr$ induced ferromagnetic coupling and eventually leads to the magnetic enhancement.

**Acknowledgements** The work was supported by the National Natural Science Foundation of China (Grant Nos. 10604013 and

20873019), the program for New Century Excellent Talents in the University of China (NCET–06–0470), the project-sponsored by SRF for ROCS, SEM, the Qinglan Project in the University of Jiangsu Province, and the Teaching and Research Foundation for the Outstanding Young Faculty and Peiyu Funding of Southeast University. The authors would like to acknowledge computational resources at the Department of Physics, Southeast University.

## References

1. J. Bansmann, S. H. Baker, C. Binns, J. A. Blackman, J. P. Bucher, J. Dorantes-Davila, V. Dupuis, L. Favre, D. Kechrakos, A. Kleibert, K. H. Meiwes-Broer, G. M. Pastor, A. Perez, O. Toulemonde, K. N. Trohidou, J. Tuaillon, and Y. Xie, Surf. Sci. Rep., 2005, 56: 189
2. C. Binns, K. N. Trohidou, J. Bansmann, S. H. Baker, J. A. Blackman, J. P. Bucher, D. Kechrakos, A. Kleibert, S. Louch, K. H. Meiwes-Broer, G. M. Pastor, A. Perez, and Y. Xie, J. Phys. D: Appl. Phys., 2005, 38: R357
3. T. Hihara, S. Pokrant, and J. A. Becker, Chin. Phys. Lasers, 1998, 294: 357
4. S. Yin, R. Moro, X. S. Xu, and W. A. de Heer, Phys. Rev. Lett., 2007, 98: 113401
5. M. B. Knickelbein, Phys. Rev. B, 2007, 75: 014401
6. J. L. Wang, G. H. Wang, X. S. Chen, W. Lu, and J. J. Zhao, Phys. Rev. B, 2002, 66: 014419
7. Q. L. Lu, L. Z. Zhu, L. Ma, and G. H. Wang, Phys. Lett. A, 2001, 350: 258
8. J. L. Yang, C. Y. Xiao, S. D. Xia, and K. L. Wang, Phys. Rev. B, 1993, 48: 12155
9. S. Ganguly, M. Kabir, S. Datta, S. Ganguly, B. Sanyal, and A. Mookerjee, Phys. Rev. B, 2008, 78: 014402
10. P. Wu, L. F. Yuan, and J. L. Yang, J. Phys. Chem. A, 2008, 112: 12320
11. N. F. Shen, J. L. Wang, and L. Y. Zhu, Chem. Phys. Lett., 2008, 467: 114
12. G. Kresse and J. Furthmuller, Phys. Rev. B, 1996, 54: 11169
13. P. E. Blöchl, Phys. Rev. B, 1994, 50: 17953
14. G. Kresse and D. Joubert, Phys. Rev. B, 1999, 59: 1758
15. J. P. Perdew, K. Burke, and M. Ernzerhof, Phys. Rev. Lett., 1996, 77: 3865
16. S. Datta, M. Kabir, S. Ganguly, and T. Saha-Dasgupta, Phys. Rev. B, 2007, 76 (1): 014429
17. A. Kant and B. J. Strauss, Chem. Phys., 1964, 41(12): 3806
18. G. L. Gutsev, M. D. Mochena, P. Jena, C. W. Bauschlicher Jr., and H. Patridge III, J. Chem. Phys., 2004, 121(14): 6785
19. G. L. Gutsev and C. W. Bauschlicher Jr., J. Phys. Chem. A, 2003, 107(23): 4755
20. P. Bobadova-Parvanova, K. A. Jackson, S. Srinivas, and M. Horoi, Phys. Rev. B, 2002, 66: 195402
21. J. L. Wang, J. Bai, J. Jellinek, and X. C. Zeng, J. Am. Chem. Soc., 2007, 129: 4410